Dimensional Changes of Nb_3Sn Rutherford Cables during Heat Treatment

E. Rochepault, P. Ferracin, G. Ambrosio, M. Anerella, A. Ballarino, A. Bonasia, B. Bordini, D. Cheng, D.R. Dietderich, H. Felice, L. Garcia Fajardo, A. Ghosh, E.F. Holik, S. Izquierdo Bermudez, J.C. Perez, I. Pong, J. Schmalzle, M. Yu

***Abstract*—In high field magnet applications, Nb_3Sn coils undergo a heat treatment step after winding. During this stage, coils expand radially and contract longitudinally due to the Nb_3Sn phase change. In order to prevent residual strain from altering superconducting performances, the tooling must provide the adequate space for these dimensional changes. The aim of this study is to understand the behavior of cable dimensions during heat treatment and to provide estimates of the space to be accommodated in the tooling for coil expansion and contraction. This paper summarizes measurements of dimensional changes on strands, single Rutherford cables, cable stacks, and coils performed between 2013 and 2015. These samples and coils have been performed within a collaboration between CERN and US LARP Program to develop Nb_3Sn quadrupole magnets for the HiLumi LHC. The results are also compared with other high field magnet projects.**

***Index Terms*—Conductor Dimensions, heat treatment, Nb_3Sn conductors, Rutherford cables.**

I. Introduction

High field magnets for the LHC luminosity upgrades require the use of the Nb_3Sn superconductor in order to achieve the desired performances in terms of magnetic field and gradient [1]. Among different fabrication steps, the coils must be reacted at 650°C during 50-100h to form the Nb_3Sn superconducting phase. Early observations on coil dimensional changes during heat treatment were made at Fermilab. A significant coil longitudinal growth was first observed and the reason was identified as a lack of room in the reaction fixture cross-section. Then it was decided to leave some transversal space in the cavity to allow the coil to expand during reaction [2]. In the LARP LQ program, a decision was made for following programs to allow the coil to contract longitudinally by means of gaps in the pole and by favoring the longitudinal sliding with the fixture [3]. Further analysis showed that the performance of first HQ coils were degraded, potentially because the tooling was designed to fit the un-reacted cable and was over-compacting the reacted coils. Whereas in the LQ coils, some room was left for transverse expansion, and they were performing better [4]. Then it was decided for the next coil generations to accommodate some room for the cables to expand transversally in the reaction fixture. For the MQXF project [5], in the framework of a collaboration between CERN and the US LARP Program, an investigation was carried out to (i) quantify the dimensional changes of conductors during reaction under different conditions (single strands, cables, coils); and (ii) estimate the consequent space to be left in the tooling for cable expansion.

II. Conductor parameters

The CERN MQXF conductor is a Rutherford cable made either of PIT 192 or RRP 132/169 strands around a 12 mm x 25 µm stainless steel core. The LARP MQXF cable is using the same configuration, with RRP 108/127 strands. A S2 glass insulation is braided around the cable prior to winding, and a ceramic binder is applied to the coil before heat treatment to provide additional mechanical stability during the fabrication process. Finally, the coils are impregnated with epoxy resin to ensure complete electrical insulation. The strand and cable parameters used at both LARP and CERN are listed in Table I.

TABLE I
MQXF 1ST GENERATION CONDUCTOR PARAMETERS

Parameter	Value	Unit
Strand Cu:Sc ratio	1.2	-
Strand diameter	0.85	mm
Number of strands	40	-
Cable twist pitch	109	mm
Un-reacted bare cable mid-thickness	1.525	mm
Un-reacted bare cable width	18.150	mm
Cable keystone angle	0.550	°
Cable insulation thickness	0.150	mm

III. Strands

The radius of several single bare strands have been measured at CERN, before and after reaction. The strands are free in all

Current version: 2/17/2016.

E. Rochepault, P. Ferracin, A. Ballarino, A. Bonasia, B. Bordini, L. Garcia Fajardo, S. Izquierdo Bermudez and J.C. Perez are with CERN, CH-1211 Geneva 23, Switzerland (e-mail: Etienne.rochepault@cern.ch).

G. Ambrosio, E. Holik, and M. Yu are with Fermi National Accelerator Laboratory, Batatvia, IL 60510 USA.

M. Anerella, A. Ghosh and J. Schmalzle are with Brookhaven National Laboratory, Upton, NY 11973 USA.

D. Cheng, D. Dietderich, H. Felice, and I. Pong are with Lawrence Berkeley National Laboratory, Berkeley, CA 94720 USA.

H. Felice is currently affiliated with CEA Saclay, 91191 Gif-sur-Yvette, France.

Research supported by EU FP7 HiLumi LHC - Grant Agreement 284404 and by the U.S. Department of Energy via the US-LARP program.

directions in this configuration, as shown in Fig. 1. The RRP strands have a radius expansion of about 1.8 % and the PIT 1.6 %. These values are comparable to measurements done on RRP strands having a similar Cu:Sc ratio [6]. This study and other experiments [7] tend to indicate that the expansion increases with superconductor content, consistent with the hypothesis that the volume expansion is due to the Nb_3Sn phase change during reaction.

The values of [7] also show that the thickness growth of rolled wires can be up to two times the radius growth of virgin wires, suggesting that part of the expansion is due to stresses accumulated during the rolling process and released during the thermal cycle. Virgin strands seem to have a tendency to expand in length as well (0.03 to 0.1 % [6]), but the contribution to the volume expansion is low. The values are summarized in Table II. Based on these data, the cross-section area expansion of un-confined strands is between 3.2 and 3.6 %, for volume expansions around 3.7 % (considering only Cu:Sc ratios of 1.2).

Fig. 1: Bare single strand used for expansion measurement.

TABLE II
AVERAGE DIMENSIONAL CHANGES OF STRANDS

Sample	Cu:Sc	Radius/Thickness expansion [%]	Length expansion [%]
MQXF RRP virgin	1.2	1.8	-*
MQXF PIT virgin	1.2	1.6	-
RRP virgin [6]	1.15	1.8	0.08
RRP virgin [6]	0.85	2.2	0.04
IT virgin [7]	0.61	1.8	-
PIT virgin [7]	0.83	2.2	-
ITER virgin [7]	1.42	0.9	-
IT rolled [7]	0.61	4.4	-
PIT rolled [7]	0.83	2.3	-
ITER rolled [7]	1.42	1.9	-

*Blank cells denote unavailable data.

IV. CABLES

A. *Single Cable*

Dimensional changes of cables were extensively measured at LBNL [8]. The samples are about 1.3 m long and are reacted between stainless steel bars which allow for expansion in all directions. Different conditions were compared: confined transversally and un-confined, sleeve insulation or braid. This study shows for instance that free cables, as opposed to free strands, have the tendency to contract in length (-0.6 to 0 %), probably due to remaining cabling tension or friction between the strands. In average, the confined cables exhibit 2.2 % expansion in cross-section area and 2.6 % in volume. The unconfined cables using a braid are around 3.4 % in area and 3.2 % in volume, whereas the unconfined cables using a sleeve are around 3.9 % and 3.5 % respectively.

In Fig. 2, the area change is plotted as a function of the length change, for these different cable measurements. The expansion behaviour seems to follow a linear trend. When confined laterally ('HQ' markers), cables expand by only the available space. Consequently, the cables expand longitudinally and the volume expansion is low. A braided insulation, tight around the cable, provides some transverse confinement and prevents part of the area expansion ('MQXF – braided' markers). Then the length contracts very little. With a sleeve insulation, looser, the cable is able to expand more in area and contract in length ('MQXF – sleeve' markers). The associated volume expansion is higher in this case. This finally shows that the transverse confinement can have a significant impact on dimensional changes. Note that no clear impact of the binder has been identified.

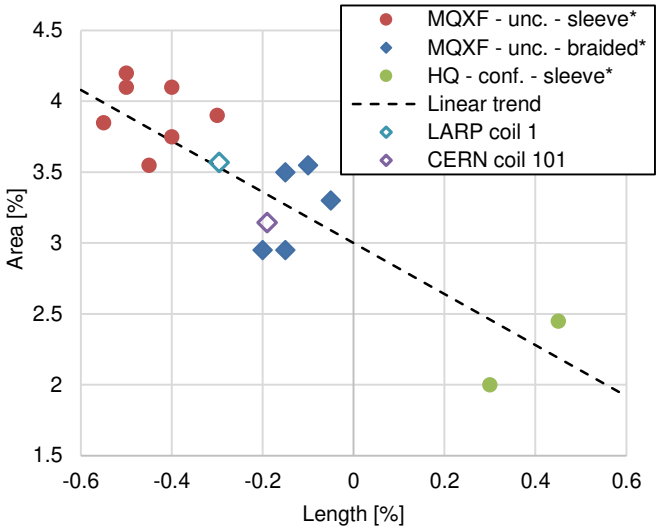

Fig. 2: Area expansion vs. length expansion for cables using sleeves or braided insulation. "Conf." stands for confined cables, "Unc." stands for un-confined cables. The values of two MXQF coils using braid are plotted with open markers for comparison (see section V for more details). *Data from *[8]*.

B. *Cable stacks*

At CERN, stacks of 10 MQXF RRP bare cables (about 200 mm long), arranged using alternate direction, have been reacted in a large cavity in order to leave room for expansion (see Fig. 3). The dimensions before and after reaction are measured with a Coordinate Measurement Machine (CMM). The RRP cables have mid-thickness and width expansions of 2.5 % and 1.7 %. PIT cables exhibit slightly different values: respectively 3.0 % and 1.5 %, for an equivalent growth in area of about 4.2-4.5 %. Note that thickness expansions are consistent to values reported in [7] for rolled wires, and that width expansions are comparable to values measured for virgin wire radii.

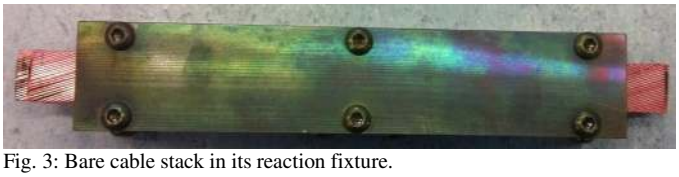

Fig. 3: Bare cable stack in its reaction fixture.

Stacks of insulated cables were also reacted in a cavity allowing 2.0 % growth in width and 4.5 % growth in thickness, as depicted in Fig. 4. The mid-thickness was measured for stacks with and without heat treatment, under a 5 MPa pressure, by recording the displacement of the press. The resulting thickness expansion is 2.5 %, which is consistent with bare cable values. Separate experiments proved that the insulation does not change its thickness during reaction. For comparison, thickness growths from 2.9 % to 3.8 % have been reported [9] for cables made of 40 strands of 1 mm diameter and 1.3 Cu:Sc

ratio, using PIT and RRP technologies. The values for single cables and cable stacks are summarized in Table III.

Fig. 4: Insulated cable stacks in the reaction fixture, before heat treatment.

TABLE III
AVERAGE DIMENSIONAL CHANGES OF CABLES

Sample	Thickness exp. [%]	Width exp. [%]	Length contr. [%]
MQXF RRP bare cable	2.5	1.7	-
MQXF PIT bare cable	3.0	1.5	-
MQXF RRP braided	2.5	-	-
MQXF unconf. sleeve [8]	2.8	1.1	-0.4
MQXF unconf. braided [8]	3.2	0.0	-0.1
HQ conf. sleeve [8]	2.1	0.1	0.4
FRESCA2 RRP 10-stack [9]	3.0	-	-
FRESCA2 PIT 10-stack [9]	3.6	-	-

V. COILS

A. *Transverse expansion*

The LARP programs has been benefiting from a lot of experience accumulated with many coils. Cables in TQ and LQ coils were allowed to expand transversally in a large cavity (1-2 % in width and ~6 % in thickness), whereas the cavity of the first HQ generation was allowing the cables to grow only by 0.8-1.3 % in width and 1.4-1.8 % in thickness [4]. For the third HQ generation, the sleeve insulation was replaced by a braided insulation and the room for expansion was increased to 1.4 % in width and 3.9 % in thickness [10].

An automated image analysis has been performed on two MQXF coil cross-section cuts (CERN 101 and LARP 1). The analysis algorithm consists in detecting the cable contours using the sharp difference in brightness between the cables and the surrounding insulation. Then the best fits are applied to the strand edges in order to encapsulate the detected contours. This method gives an average value and, because of a 'barrel' shape sometimes observed, may slightly differ from other methods measuring directly thin and thick edges of the cable [11]. The four obtained lines are used to build the position of the four corners of the cable (see Fig. 5). Finally, different reference lengths are used to scale the dimensions from pixels to mm. This method was validated on the CERN coil 101, using a tri-dimensional measuring machine, and was compared with other measurements on the LARP coil 1 [11].

The values from cross-section analysis are summarized in Table IV. The amount of data is sufficient to allow statistical analysis and estimate the standard deviations. Thickness expansions of about 3 % and width expansions between 0 and 0.5 % have been found, which correspond to cross-section area expansions from 2.9 to 3.6 %. These values are consistent with measurements on cables with braided insulation [8], but the width expansion is lower than the measured value (see Table III). However, these expansions are less than the 4.5 % and 2 % initially expected. Consequently, for the second generation of coils, the cavity size has been redesigned to accommodate for this lower expansion [12].

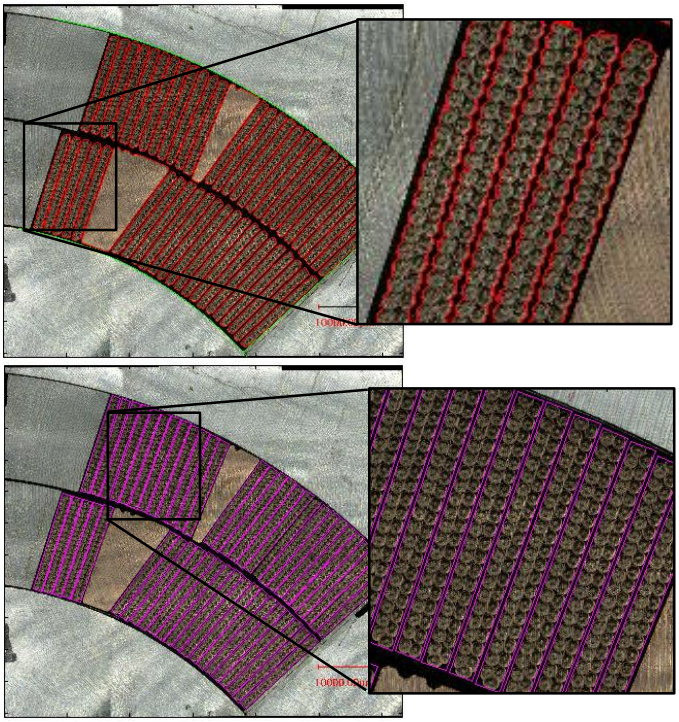

Fig. 5: Image analysis of a MQXF coil cross-section. Top: Contour detection; Bottom: Trapezoid fits.

TABLE IV
COIL X-SECTION ANALYSIS

Coil	Method	Thickness expansion [%]	Width expansion [%]
CERN 101	3D measurement machine	3.0 +/- 1.3	0.14 +/- 0.15
	Image analysis	2.9 +/- 1.3	0.04 +/- 0.17
LARP 1	Laser confocal scope [11]	3.1 +/-	0.45 +/-
	Image analysis	3.3 +/- 1.3	0.12 +/- 0.16

B. *Longitudinal Contraction*

In the HQ program, based on the considerations described above, some gaps were accommodated in the pole parts to allow the coils to contract after releasing the winding tension and after reaction. It was demonstrated that the type of cable insulation had a significant impact on the contraction. Total contractions between -0.4 and -0.3 % were reported for coils using sleeves, and around -0.2 % for braided insulations [10].

The gaps for MQXF coils are systematically measured: before winding, after curing, before heat treatment, and after heat treatment, as depicted in Fig. 6. Up to now, 4 RRP and 2 PIT coils have been reacted at CERN and 6 RRP coils at LARP. Cumulated contractions between -0.3 and -0.1 % were measured [13] and are summarized in Fig. 7. The contribution of contraction during curing is -0.03 % on average. It is interesting to notice that the CERN Cu coil 000 had a significant contraction during reaction, suggesting that any coil will

naturally contract because of winding tension, and that the longitudinal expansion of Nb_3Sn compensates for some of this contraction. Since area and length change are available for coils CERN 101 and LARP 1, the corresponding values have been added in Fig. 2, and are in good agreement with data on unconfined braided cables.

Fig. 6: Gaps in the pole at different steps. Top left: gaps set with controlled shims. Top right: gap remaining after release of the winding tension. Bottom: gaps almost closed after reaction.

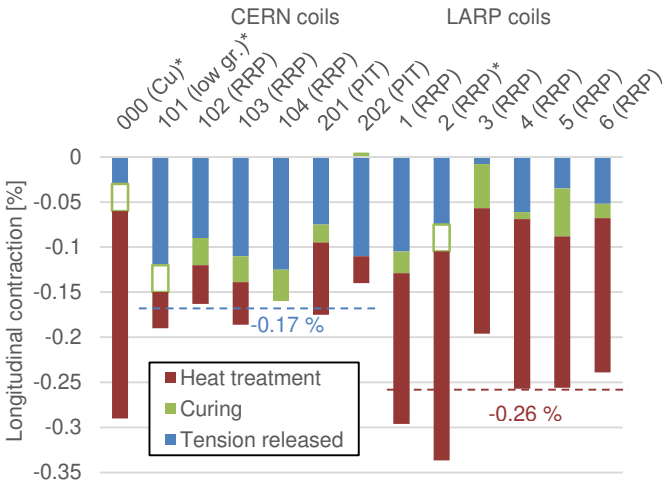

Fig. 7: Longitudinal contraction of MQXF CERN and LARP coils *[13]*, after tension release, curing and heat treatment. The average total contraction is indicated on the plot. *For these coils, no data were available on the contraction during curing. A contraction of -0.03 % is then assumed (open bars), the total being conserved.

In Fig. 8, the longitudinal contractions from these different studies are compared by plotting the length change after reaction as a function of the length change after winding. The graph first shows that HQ02 coils, using sleeves, have a higher range of contraction than the other coils, using braided insulations, which was already pointed out in Fig. 2. One can notice also that the contraction during reaction is inversely proportional to the contraction after winding, with a factor close to 1, suggesting that the remaining tension that was not released after winding will be released during reaction. Lines corresponding to $\Delta L_{reac.} + \Delta L_{wind.} = constant$ are plotted for comparison. HQ02 for instance, with the sleeves, exhibit average total contractions around -0.37 %. The behavior of MQXF CERN coils, with total contractions of -0.17 % on average, is very similar to HQ03 coils. However, MQXF LARP coils are not following this trend, potentially because the coils cannot expand or contract as they would like during reaction. The reason of this behavior could be explained by different braiding parameters between LARP and CERN. This could have a significant impact on the pressure applied by the insulation to the cable, and LARP MQXF insulation could apply less transverse pressure to the cable as compared to the CERN insulation [11]. Another study has been carried out on small racetracks, using PIT and RRP cables in different conditions [9]. It is shown for instance that bare cables contract by -0.6 % on average whereas braided cables (same braid used for MQXF CERN cables) contract by -0.2 % on average. Moreover, a test done with a bare cable on an iron pole showed that the contraction was already -0.4 % at 190°C, then -0.7 % at 400°C, for a final contraction of -0.8 % at the end of the thermal cycle. These observations tend to indicate that the contraction is due to a stress release and occur mostly before the Nb_3Sn phase change, rather associated with a volume expansion. Consequently, higher contractions have been measured for racetracks wound on iron poles, compared to racetracks wound on Ti poles. This is likely due to the higher thermal dilation of the iron, preventing part of the coil contraction during ramp up to 650°C.

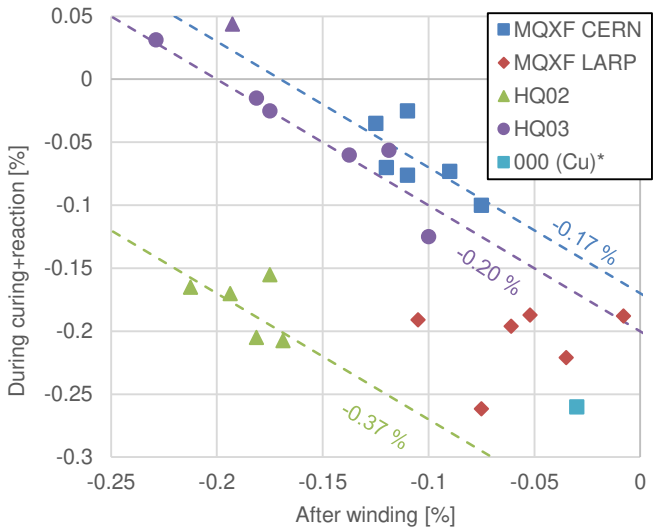

Fig. 8: Longitudinal contraction of coils in different programs. Linear trends use a slope equal to one. The corresponding values of total contraction are indicated on the lines. The contractions during curing and reaction are added for an easier comparison with available data on HQ. HQ02 coils used sleeve insulations whereas HQ03 and MQXF use braided insulations. Note that HQ coil 17, part of the HQ02 generation but using a braid, has been plotted with HQ03 coils (purple triangle marker).

TABLE V
SUMMARY OF AVERAGE DIMENSIONAL CHANGES FOR CABLES AND COILS

Conductor	Insula -tion	Thick. [%]	Width [%]	Length [%]	Area [%]	Vol. [%]
MQXF cable	Sleeve	2.8	1.1	-0.4	3.9	3.5
	Braid	3.2	0.0	-0.1	3.2	3.1
CERN 101	Braid	3.0	0.1	-0.04	3.1	3.0
LARP 1	Braid	3.1	0.5	-0.2	3.6	3.4

VI. Conclusion

An overall volume dilatation of Nb_3Sn during reaction of about 4 % has been observed for unconstrained strands. This expansion is exhibited mainly in the transverse direction. Note that the influence of strand technology (PIT, RRP…) is not significant. However, in Rutherford cables, the compaction of the strands, the remaining stress, the friction between strands, and with the surrounding insulation, can lead to different longitudinal contractions. For instance, the fiber-glass sleeves, slit on the cables, are potentially looser than fiber-glass tightly braided on the cables, allowing the cable to expand more transversally and contract more longitudinally. With sleeve insulations, cables expand between 3.5 and 4.2 % in cross-section area and contract between -0.6 and -0.3 % in length, whereas for braided insulations, the dimensional changes are about 3 to 3.5 % in area and -0.2 to 0 % in length. Inside coils, the conditions are even more stringent. Since it was suggested in previous projects that the transversal over-compaction was a potential cause of degraded performances, some room have been accommodated in reaction tooling to let the cable expand during reaction. The expansions measured in MQXF coil cross-section are about 3 % in thickness and 0 % in width, which is consistent to other observations made on cables with braided insulation. Moreover, cables are submitted to additional remaining stresses due to winding and, even though a contraction after winding is often observed, the contribution of remaining stress release during thermal cycle is difficult to quantify. Anyways, the total contraction of MQXF coils after reaction is around -0.1 %, which is in agreement with the measurements done on cables using a braided insulation. Finally, as summarized in Table V, MQXF coils contract between 3.1 and 3.6 % in area, for a corresponding volume expansion around 3.0 to 3.4 %. These values are consistent with measurements done on unconfined cables.

Acknowledgment

The authors would like to thank A. T. Perez Fontenla for taking a lot of time and a great care in the coil cross-section images acquisition. E. F. Holik and I. Pong gratefully acknowledge the support of the Tim Toohig Fellowship in Accelerator Science from the US LHC Accelerator Research Program.

References

[1] E. Todesco et al., "A First Baseline for the Magnets in the High Luminosity LHC Insertion Regions," *IEEE Trans. Appl. Supercond.,* vol. 24, no. 3, p. 4003305, 2014.

[2] D. R. Chichili et al., "Fabrication of the Shell-type Nb_3Sn Dipole Magnet at Fermilab," *IEEE Trans. Appl. Supercond.,* vol. 11, no. 1, pp. 2160-2163, 2001.

[3] G. Ambrosio et al., "Development and Coil Fabrication for the LARP 3.7-m Long Nb_3Sn Quadrupole," *IEEE Trans. Appl. Supercond.,* vol. 19, no. 3, pp. 1231-1234, 2009.

[4] H. Felice et al., "Impact of Coil Compaction on Nb_3Sn LARP HQ Magnet," *IEEE Trans. Appl. Supercond.,* vol. 22, no. 3, p. 4001904, 2012.

[5] P. Ferracin et al., "Development of MQXF, the Nb_3Sn Low-β Quadrupole for the Hi-Lumi LHC," *IEEE Trans. Appl. Supercond.,* submitted for publication.

[6] D. Bocian, G. Ambrosio and G. M. Whitson, "Measurements of Nb_3Sn Conductor Dimension Changes During Heat Treatment," *AIP Conf. Proc. 1435, 193 (2012); http://dx.doi.org/10.1063/1.4712096* .

[7] N. Andreev, E. Barzi, D. Chichili, S. Mattafirri and a. A. Zlobin, "Volume Expansion of Nb-Sn Strands and Cables During Heat Treatment," *Adv. in Cryogenic Eng.,* vol. 17, no. 2, pp. 2607-2610, 2007.

[8] I. Pong, D. R. Dietderich and A. Gosh, "Dimensional Changes of Nb_3Sn Cables during Heat Treatment," *Presented at ICMC 2015.*

[9] M. Durante et al., " Nb_3Sn Rutherford cables geometrical behavior during heat treatment," *IEEE Trans. Appl. Supercond.,* submitted for publication.

[10] F. Borgnolutti et al., "Fabrication of a Third Generation of Nb_3Sn Coils for the LARP HQ03 Quadrupole Magnet," *IEEE Trans. Appl. Supercond.,* vol. 25, no. 3, p. 4002505, 2015.

[11] T. Holik et al., "Fabrication and Analysis of 150 mm Aperture Nb_3Sn MQXF Coils," *IEEE Trans. Appl. Supercond.,* submitted for publication.

[12] S. Izquierdo Bermudez et al., "Second Generation Coil Design of the Nb_3Sn low-B Quadrupole for the High Luminosity LHC," *IEEE Trans. Appl. Supercond.,* submitted for publication.

[13] M. Yu, Private communication*,* 2015.